

Structure of Motion-Sensitive Synaptic Terminals in the Mouse Lateral Geniculate Nucleus

Hays Johnson
McGill University

April 2022

In this project, I investigated the structure and selectivity of the synaptic terminals from the LGN to V1 region of the mouse visual cortex. While receptive fields and direction selectivity have been shown to be present within the LGN, it is not known what if any larger-scale structure exists to encode this information as it is transferred to the visual cortex. Using 2P calcium imaging data recorded by Dr. Erik Cook, I found the maximum response to different motion stimuli for each ROI, averaged over each trial. Using these data I was able to sort the synapses by response type to develop density plots and visualize the underlying structure. My results show that responsive ROIs do differ by stimulus type, evidencing direction and ON/OFF selectivity in LGN synaptic terminals. However, this selectivity did not appear to create a noticeable structure. Further research is needed to establish whether or not such a structure exists.

1 Introduction

This project investigated the link between organizational structure and motion/direction selectivity in the axons of the thalamic lateral geniculate nucleus (LGN) and their synaptic terminals onto the primary visual cortex (V1). Both the LGN and V1 are essential parts of mammals' visual processing circuitry. The LGN, known as "the gateway to the visual cortex"[9], is the mediator and

thalamic relay between visual information traveling along the optic nerve and V1. It is the first step in visual processing and feature selection, but it has been difficult to know to what degree this processing occurs, as small receptive fields (RFs) and eye movements make precise study of the LGN difficult[9]. It was previously thought that the LGN encoded only simple center-surround RFs, and that more advanced feature selection occurred further downstream[8]. However, Piscopo et al. showed that the LGN contains many direction- and orientation-selective neurons whose input can be traced directly from the retina, evidencing an elaborate visual representation in the LGN[8].

V1 is another brain region whose full role in visual processing is still under investigation. V1 is organized in six functionally distinct layers, and is known to represent a 2D retinotopic map, presenting visual stimuli faithful to their size and spacial layout on the retina[5]. V1 also encodes much more information about visual stimuli, including orientation, eye of origin, and direction of motion[5]. However, less is known about its connections with the LGN, the function of each layer, and V1's precise role in perception. While widely thought that the LGN projected only superficially to the first layer of V1, it has now been shown that the LGN synapses extensively with Layers 2 and 3 of V1[11]. These layers are also known to play a major role in direction selectivity and motion perception[6]; these findings combined with Piscopo et al.'s paint a convincing picture of elaborate feature selection in the LGN and its direct role in motion processing in V1.

While these are much-studied areas of the brain, to my knowledge no one has looked at the organizational structure of LGN-V1 synapses and the role it may play in direction selectivity and motion perception. Working with Dr. Erik Cook of McGill University and using data collected by him, I analyzed synaptic terminal responses to various stimuli to visualize said structure and try to determine if it has a role in motion perception.

2 Methods

All data were recorded by Dr. Erik Cook at McGill University. Mice in fixed-head tasks were displayed stimuli from two screens, one in front of each eye. Two types of stimuli were present in the experiment. In the motion stimulus condition, a random dot kinematogram was divided into 216 patches, which each moved coherently in one of four randomly chosen directions (0° , 90° , 180° , and 270°) for 60 frames, whose starting time was also determined randomly.

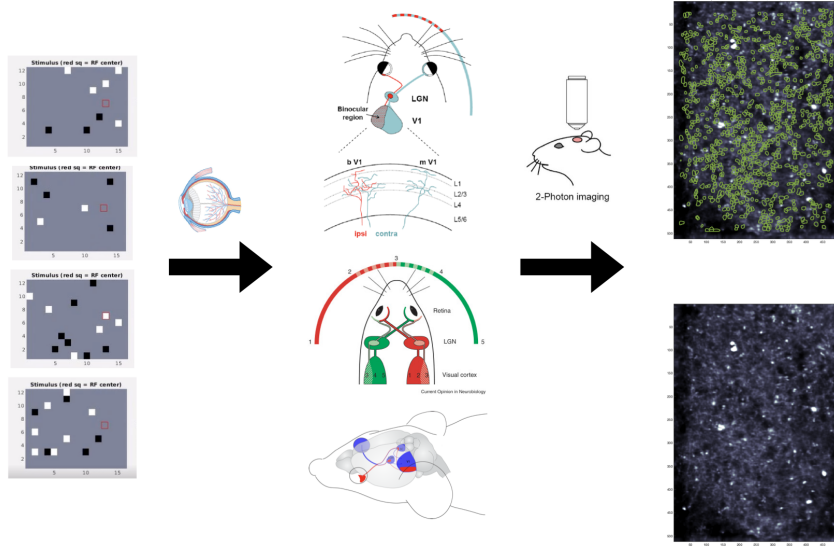


Figure 1: An example sparse noise trial. The sparse noise stimuli shown on the left are displayed to the mouse, whose neural activity is recorded via 2P calcium imaging. The average image of the brain activity throughout the experiment is shown on the bottom right, while the image above has the boundaries of responsive ROIs to black & white sparse noise overlaid on top.[1][2][3][4][10]

At the end of each motion trial, a global motion event occurred where all dots moved in one direction for 61 frames. In the sparse noise stimulus condition, 192 patches flashed from gray to either black or white, randomly chosen, for a duration of 30 frames. The experiment was split into 153 trials, which were grouped in blocks of four: three motion trials and one sparse noise trial. The ordering of the sparse noise trial in the group of four was determined randomly. The mice were recorded using two-photon calcium imaging with a 130x130 micron field of view to capture neural activation during the experiment. An example sparse noise trial is shown in Figure 1.

Data analysis was performed in MATLAB, with data preprocessing and some functions provided by Dr. Cook. The raw fluorescence image data captured in 2P recording was used to identify and mark 3405 regions of interest (ROIs) using suite2p[7]. Each ROI represents an LGN axon synapsing on V1. The raw fluorescence was first normalized using a z-score: subtracting the signal mean from the signal and dividing by the standard deviation. In this analysis, both

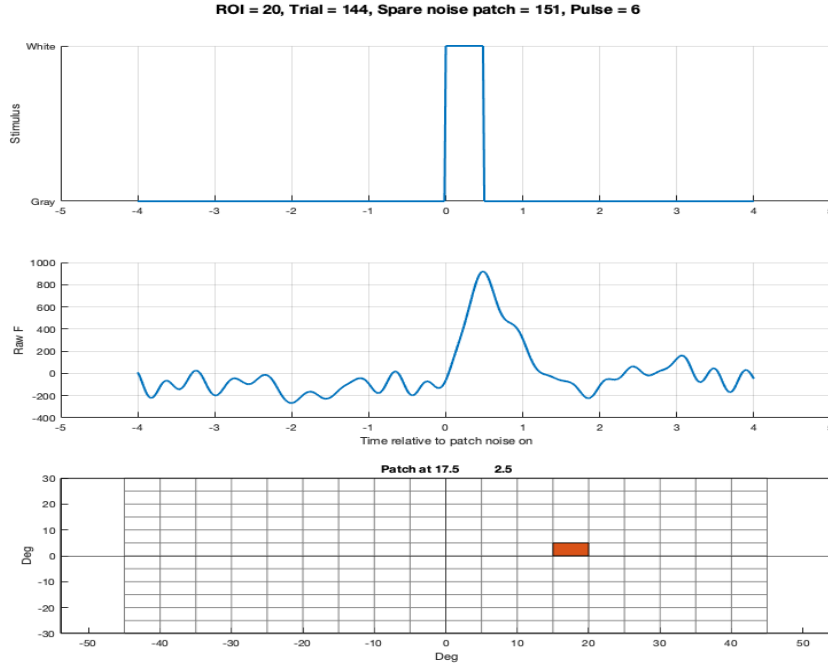


Figure 2: A single ROI response to sparse noise. The raw fluorescence signal (middle) is aligned with the white stimulus onset (top) occurring in patch 151 (bottom).

the mean and standard deviation were calculated using a window of one trial on each side. Then, I aligned each ROI response to each stimulus at each patch, as shown in figure 2. Responses were separated and stored based on stimulus type: for sparse noise, by black vs. white noise, and for patch motion and global motion, by coherent motion direction. These responses were averaged over all trials, per patch. I found the patch whose stimuli produced the largest response and used this response as the ROI's maximum overall response. This controlled for RFs in deciding which stimulus type maximally activated each ROI.

Each ROI was grouped according to this maximum response. For sparse noise, ROIs were separated into three groups: responsive to only black patch noise, responsive to only white patch noise, and responsive to both. For the motion trials, ROIs were grouped according to responsive direction, and only included if they did not respond to any other motion direction. Responsive was defined as a z-score greater than or equal to 0.5. To further normalize, a mean was

calculated using the two seconds prior to stimulus onset and subtracted from the entire signal. This brought each signal to baseline and ensured the z-score cutoff would be applied more evenly. Unresponsive ROIs were omitted from analysis.

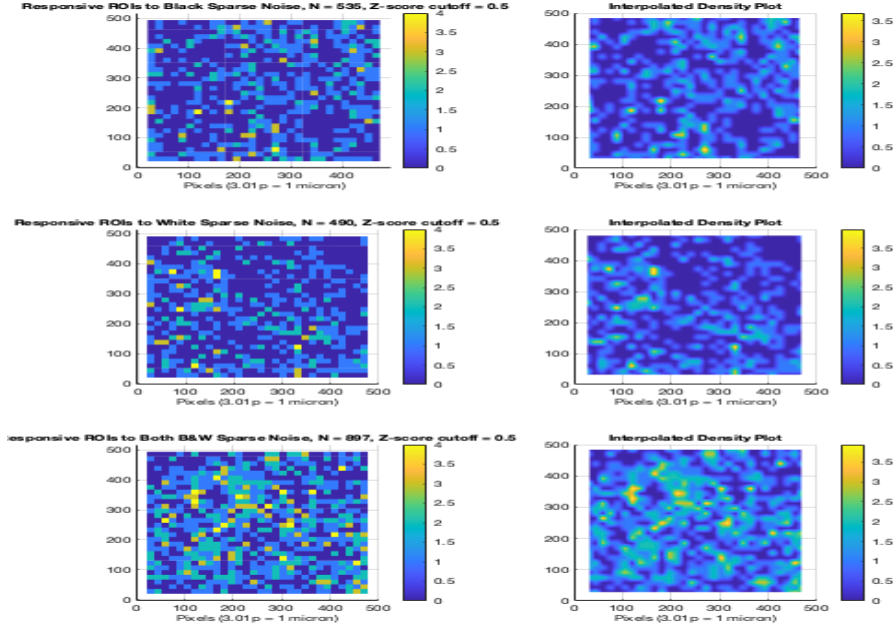


Figure 3: Sparse Noise Responses

3 Results

My results consisted mainly of numerical ROI responses and subsequent graphical analysis, performed in MATLAB. These results represent a comprehensive analysis of each ROI's maximum response to each stimulus type: for the sparse noise condition, all responses over $z = 0.5$ and respective ROI indices were stored, while in the motion conditions, all responses were stored for each direction, indexed by ROI number and separated by patch vs. global motion. To visualize the structure and distribution of the ROIs, I used the ROI pixel boundaries on the average image of the experiment and calculated the center of

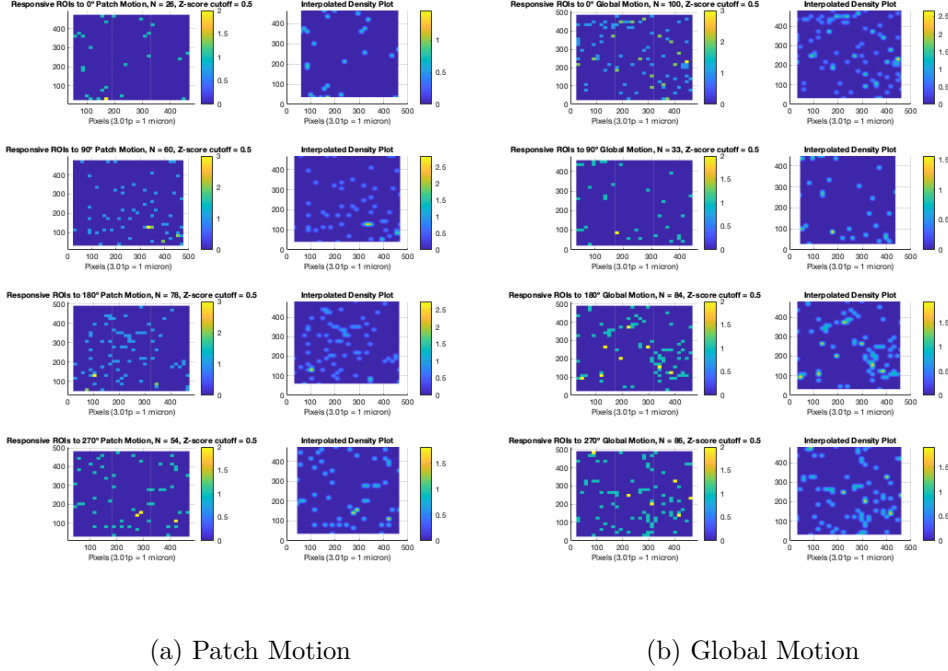


Figure 4: Motion Responses

each polygon contained by the ROI perimeter. I then stored and binned these ROI centers in a 30x30 2D histogram overlaid on the 130x130 micron average image. The data was also linearly interpolated and plotted side-by-side with the histograms to provide a clearer picture of the ROIs' structure, as can be seen in Figures 3 and 4.

Many ROIs responded above the z-score threshold for multiple types of stimuli. In the sparse noise case, this was not an issue, as there were still hundreds of ROIs that responded only to black or white stimuli; furthermore, it was easy to plot ROIs responsive to both conditions as there *were* only two conditions. The motion cases were different. Because ROIs were only included if they responded to *only* one of the four motion directions, each direction represented an average of 55 ROIs for patch motion and 76 for global; some directions, as few as 26 or 33 ROIs. While these criteria were chosen to best visualize the general structure of the direction selectivity of the ROIs, and was successful to that end, further research into this question would be illuminating. Several ROIs responded above threshold to all motion directions, and many responded

strongly to motion in the *opposite* direction as its primary responsive direction. Grouping ROIs along these trends may reveal results this research did not.

4 Discussion and Conclusion

Ultimately, no discernable structure was found to account for direction selectivity and motion perception in LGN-V1 synaptic terminals. The motion stimuli plots are visually quite sparse, and show no obvious pattern in the layout of their ROIs. The sparse noise stimulus produced denser plots, with more responsive ROIs, but they too did not seem to display any noticeable pattern or structure besides a few ROI clusters dispersed throughout. To further investigate the LGN synaptic structure, I propose grouping the ROIs differently to see if any new trends emerge. For example, while response-per-patch data were used to identify each ROI's RF and thus maximum response, this location information is not present in the final density plots. Perhaps visualizing ROIs by RF instead of by orientation of direction selectivity would provide a clearer structure. Also, as mentioned above, many ROIs exhibited responses to motion in a given direction as well as in the opposite direction; that is, responsive to both 0° and 180° motion or 90° and 270° . Including ROIs with these opposite responses as well could be another interesting variation. Given the time constraints of this project the above experiments could not be performed, but further investigation into responses to all direction and their combinations could also provide interesting further results.

This research did support the belief that elaborate feature selection and RFs exist in the LGN and its projections to V1. Most if not all ROIs had a select number of patches that produced any response, demonstrating strong RF selectivity. As can be seen in Figure 2, even one showing of a patch stimulus produced strong responses in several ROIs, given that the stimulus was in said ROI's receptive field.

While this project did not present strong findings regarding the organizational structure of the LGN's synaptic terminals with respect to motion selectivity, it did support several previous findings on the LGN's role in visual perception. Furthermore, it provided a successful way to analyze ROI data both numerically and visually, which can be used in further investigations.

Acknowledgements

I would like to thank Dr. Erik Cook for agreeing to supervise me for this project; for his mentorship and advice in our meetings; and for the code, data, and support he provided me to conduct this research.

References

- [1] Daniel Cole. Anatomy of human eye illustration, 2018. [Online; first accessed from Alamy.com on January 24, 2022].
- [2] BioImaging Group. 2-photon calcium imaging, 2021.
- [3] Sonja B. Hofer. Imaging development and plasticity in the mouse visual system. 2006.
- [4] Mark Hübener. Mouse visual cortex. *Current Opinion in Neurobiology*, 13(4):413–420, 2003.
- [5] Michael Ibbotson and Young Jun Jung. Origins of functional organization in the visual cortex. *Frontiers in Systems Neuroscience*, 14, 2020.
- [6] T. Marques, M. T. Summers, G. Fioreze, M. Fridman, R. F. Dias, M. B. Feller, and L. Petreanu. A role for mouse primary visual cortex in motion perception. *Current biology : CB*, 28(11):1703–1713.e6, 2018.
- [7] Marius Pachitariu, Carsen Stringer, Mario Dipoppa, Sylvia Schröder, L. Federico Rossi, Henry Dalgleish, Matteo Carandini, and Kenneth D. Harris. Suite2p: beyond 10,000 neurons with standard two-photon microscopy. *bioRxiv*, 2017.
- [8] D. M. Piscopo, R. N. El-Danaf, A. D. Huberman, and C. M. Niell. Diverse visual features encoded in mouse lateral geniculate nucleus. *The Journal of neuroscience : the official journal of the Society for Neuroscience*, 33(11):4642–4656, 2013.
- [9] John H. Reynolds, Jacqueline P. Gottlieb, and Sabine Kastner. Chapter 46 - attention. In Larry R. Squire, Darwin Berg, Floyd E. Bloom, Sascha du Lac, Anirvan Ghosh, and Nicholas C. Spitzer, editors, *Fundamental Neuroscience (Fourth Edition)*, pages 989–1007. Academic Press, San Diego, fourth edition edition, 2013.

- [10] Tenelle A. Wilks, Alan R Harvey, and Jennifer Rodger. Seeing with two eyes: Integration of binocular retinal projections in the brain. 2013.
- [11] Jun Zhuang, Yun Wang, Naveen D. Ouellette, Emily Turschak, Rylan S. Larsen, Kevin T. Takasaki, Tanya L. Daigle, Bosiljka Tasic, Jack Waters, Hongkui Zeng, and R. Clay Reid. Motion/direction-sensitive thalamic neurons project extensively to the middle layers of primary visual cortex. *bioRxiv*, 2021.